Virologica Sinica 37 (2022) 796–803

Contents lists available at ScienceDirect

Virologica Sinica

journal homepage: www.keaipublishing.com/en/journals/virologica-sinica
www.virosin.org

Research Article

Increased pathogenicity and aerosol transmission for one SARS-CoV-2 B.1.617.2 Delta variant over the wild-type strain in hamsters

Xinghai Zhang [a,*,1], Shaohong Chen [a,b,1], Zengguo Cao [a,1], Yanfeng Yao [a,1], Junping Yu [a,1], Junhui Zhou [a,b], Ge Gao [a], Ping He [a,b], Zhuo Dong [c], Jie Zhong [c], Jing Luo [c], Hongping Wei [a,*], Huajun Zhang [a,*]

[a] State Key Laboratory of Virology, Key Laboratory of Special Pathogens and Biosafety, Wuhan Institute of Virology, Chinese Academy of Sciences, Wuhan, 430071, China
[b] University of Chinese Academy of Sciences, Beijing, 101409, China
[c] Hubei International Travel Healthcare Center (Wuhan Customs Port Outpatient Department), Wuhan, 430040, China

ARTICLE INFO

Keywords:
SARS-CoV-2
B.1.617.2 Delta variant
Syrian hamsters
Pathogenicity
Transmission

ABSTRACT

During the two-year pandemic of coronavirus disease 2019 (COVID-19), its causative agent, severe acute respiratory syndrome coronavirus 2 (SARS-CoV-2), has been evolving. SARS-CoV-2 Delta, a variant of concern, has become the dominant circulating strain worldwide within just a few months. Here, we performed a comprehensive analysis of a new B.1.617.2 Delta strain (Delta630) compared with the early WIV04 strain (WIV04) *in vitro* and *in vivo*, in terms of replication, infectivity, pathogenicity, and transmission in hamsters. When inoculated intranasally, Delta630 led to more pronounced weight loss and more severe disease in hamsters. Moreover, 40% mortality occurred about one week after infection with 10^4 PFU of Delta630, whereas no deaths occurred even after infection with 10^5 PFU of WIV04 or other strains belonging to the Delta variant. Moreover, Delta630 outgrew over WIV04 in the competitive aerosol transmission experiment. Taken together, the Delta630 strain showed increased replication ability, pathogenicity, and transmissibility over WIV04 in hamsters. To our knowledge, this is the first SARS-CoV-2 strain that causes death in a hamster model, which could be an asset for the efficacy evaluation of vaccines and antivirals against infections of SARS-CoV-2 Delta strains. The underlying molecular mechanisms of increased virulence and transmission await further analysis.

1. Introduction

Coronavirus disease 2019 (COVID-19), declared a pandemic by the World Health Organization in March 2020 (Cucinotta and Vanelli, 2020), has resulted in significant human disease, death, and economic loss. As of September 4, 2022, over 600 million people worldwide have been infected and over 6.4 million people have died (World Health Organization, 2022a). The pathogen, severe acute respiratory syndrome coronavirus 2 (SARS-CoV-2), has been accumulating various mutations while circulating globally in the human population for two years (Konings et al., 2021). Based on the potential or known impact of the constellation of mutations on the phenotypic changes, including the severity of disease, transmission efficiency, and effectiveness of medical countermeasures, some evolutionary lineages such as Alpha, Beta, Gamma, and Delta were classified as variants of concern (VOCs) by World Health Organization (2022b).

The Delta variant (also known as lineage B.1.617.2), first detected in India, is characterized by carrying T19R, G142D, 156del, 157del, R158G, L452R, T478K, D614G, P681R, and D950N mutations in spike glycoprotein (Chakraborty et al., 2021). With 40%–60% more transmissibility than Alpha, as predicted by epidemiological studies, the Delta variant has swept the globe and, in a matter of months, has replaced Alpha as the predominant strain (Allen et al., 2022). The Delta variant may be 225% as transmissible as the original strain with a mean R0 of 5.08, which is much higher than the R0 of the ancestral strain of 2.79 (Dagpunar, 2021; Earnest et al., 2022; Liu and Rocklöv, 2021). People infected with the Delta variant have a shorter incubation period and a higher viral load than those infected with the earlier variants (Li

* Corresponding authors.
E-mail addresses: zhangxh@wh.iov.cn (X. Zhang), hpwei@wh.iov.cn (H. Wei), hjzhang@wh.iov.cn (H. Zhang).
[1] Xinghai Zhang, Shaohong Chen, Zengguo Cao, Yanfeng Yao, and Junping Yu contributed equally to this work.

https://doi.org/10.1016/j.virs.2022.09.008
Received 17 February 2022; Accepted 26 September 2022
Available online 29 September 2022
1995-820X/© 2022 The Authors. Publishing services by Elsevier B.V. on behalf of KeAi Communications Co. Ltd. This is an open access article under the CC BY-NC-ND license (http://creativecommons.org/licenses/by-nc-nd/4.0/).

et al., 2022). Additionally, it has been stated that the Delta variant may increase the likelihood of hospitalization (Twohig et al., 2021). A retrospective cohort study has revealed that the Delta variant is more virulent (Fisman and Tuite, 2021).

Several animal models were promptly evaluated for their sensitivity to SARS-CoV-2. The golden hamster model accurately recapitulates the virological, immunological, and pathological findings of the majority of mild to moderate human infections, which makes the hamster an excellent model to evaluate the transmissibility of SARS-CoV-2 and related newly emerging variant viruses (Chan et al., 2020; Imai et al., 2020; Sia et al., 2020; Port et al., 2021). The non-lethal hamster model has been readily available for basic and translational studies on COVID-19.

Except for the mouse model, there is no physiological small-animal model of COVID-19 with severe disease and death (Sun et al., 2020, 2021; Huang et al., 2021). Infected hamsters show pathological lung abnormalities such as pulmonary edema and consolidation along with signs of interstitial pneumonia (Rosenke et al., 2020). However, hamsters fail to develop diffuse alveolar disease and acute respiratory distress, which are found in severe human cases (Rosenke et al., 2020; Lee and Lowen, 2021). According to Mohandas et al., the Delta variant induces lung disease of moderate severity in about 40% of 8–10-week-old female hamsters (Mohandas et al., 2021). In this study, we characterized a newly isolated Delta strain (Delta630) in a hamster model relative to the early strain WIV04. We showed that the variant Delta630 was more pathogenic in animal models than previously circulating WIV04 strain and even other Delta strains. In 4–6-week-old hamsters, Delta630 caused a very severe disease with significant weight loss, and importantly, it led to 40% mortality. In two independent competitive aerosol transmission experiments, we further demonstrated that Delta630 exhibited higher replication over WIV04.

2. Materials and methods

2.1. Virus and cells

The SARS-CoV-2 WIV04 strain (IVCAS 6.7512) was originally isolated from a COVID-19 patient in 2019 (GISAID, accession no. EPI_ISL_402124) (Zhou et al., 2020). The SARS-CoV-2 Delta strain 630 (Delta630) was isolated from a swab sample of a 33-year-old man traveling from Indonesia to Wuhan in June 2021 (NGDC databases, accession no. GWHBEBW01000000). SARS-CoV-2 Delta variants Delta84 (IVCAS 6.7584) and Delta85 (IVCAS 6.7585) strains were originally isolated from a COVID-19 patient in 2019 and stored at the Wuhan Institute of Virology, Chinese Academy of Science. All amino acid variants observed in the protein sequences between the SARS-CoV-2 strains used in this study are summarized in Supplementary Table S1. Compared with the reference strain WIV04 strain, the Delta630 variants have nine amino acid substitutions in the S protein. Although the Delta630 variant shares 15 substitutions with Delta84 and Delta85, Delta630 possesses two amino acid changes not found in Delta84 and Delta85. The amino acid changes T678I in nsp3 and T120V in nsp6 were present in the Delta630 sequence as additional mutations. The deletion at residues 119–120 in the ORF8 protein of Delta630 was found, which was absent in the Delta84 and Delta85 sequences. These mutations imply that the Delta variants may vary in terms of their ability to replicate, pathogenicity, and transmissibility.

Both viruses were propagated in Vero E6 cells (ATCC® CRL-1586™) with Dulbecco's modified Eagle's medium (DMEM, Thermo Fisher) supplemented with 2% fetal bovine serum (FBS), 1 mmol/L L-glutamine, 100 IU/mL penicillin, and 100 μg/mL streptomycin. Huh-7 cells were maintained in the same medium as above, while Calu-3 cells were maintained in MEM (Gibco) instead of DMEM.

2.2. Plaque assay

A plaque assay, with a minor change to the prior description, was used to determine the virus titer (Zhang Q. et al., 2020). Briefly, virus samples were serially 10-fold diluted in DMEM containing 2.5% FBS before being inoculated onto Vero E6 cells that had been seeded overnight at 1.5×10^5/well in 24-well plates. After 1 h of incubation at 37 °C, the inoculate was changed to DMEM containing 2.5% FBS and 0.9% carboxymethyl-cellulose. Three days later, the plates were dyed with 0.5% crystal violet after being fixed with 8% paraformaldehyde. Virus titer was calculated with the dilution gradient with 10–100 plaques.

2.3. Real-time RT-PCR

Viral RNA in the nasal wash, throat swab, and tissue homogenates was quantified by one-step real-time RT-PCR as described before (Feng et al., 2020). Briefly, viral RNA was purified using the QIAamp Viral RNA Mini Kit (Qiagen) and quantified with HiScript® II One Step qRT-PCR SYBR® Green Kit (Vazyme Biotech Co., Ltd) with the primers ORF1ab-F (5′-CCCTGTGGGTTTTACACTTAA-3′) and ORF1ab-R (5′-ACGATTGTGCATCAGCTGA-3′). The amplification procedure was set up as follows: 50 °C for 3 min, 95 °C for 30 s followed by 40 cycles consisting of 95 °C for 10 s, 60 °C for 30 s. The primers used to measure the expression level of cytokines in the lung tissues of the infected animals are shown in Supplementary Table S2.

2.4. Animal infection

Animal infection was conducted in the animal biosafety level 3 (ABSL-3) facility at Wuhan Institute of Virology, with a protocol approved by the Laboratory Animal Ethics Committee of Wuhan Institute of Virology, Chinese Academy of Sciences. Hamsters (females, 4–6 weeks old) were purchased from Vital River and allowed to acclimate for a minimum of three days. They were intranasally infected with the indicated dose of WIV04 or Delta630 in a total volume of 100 μL. As part of our daily routine, we measured the body weight, and took nasal wash and throat swabs every day following infection. The lungs, nasal turbinates, and tracheas of three hamsters were taken to determine the viral loads at 3 and 7 days after infection (dpi), and lung tissue was fixed with 10% neutral formaldehyde for hematoxylin and eosin (H&E) staining.

2.5. Competitive airborne transmission experiment

Three hamsters were infected with 10^4 PFU of the 1:1 mixture of WIV04 and Delta630. The next day, the infected animals (donors) were put into one end of a cage that was divided into two ends with a stainless-steel-wired divider of 4 cm double layers. Three naïve hamsters (sentinels) were placed at the other end of the cage. An hour later, the donor and sentinel animals were transferred to new cages. Nasal wash was collected one day after infection or exposure. To determine the percentage of WIV04 and Delta630 in each animal, a 786-bp long fragment of the *S* gene was amplified with the primers S-F (5′-TCACACGTGGTGTTTATTACCCT-3′) and S-R (5′GAGGGTCAAGTGCACAGTCT-3′) using TransStart® FastPfu DNA Polymerase (TransGen Biotech Co., LTD), and cloned into pEASY®-Blunt Cloning Kit (TransGen Biotech Co., LTD). At least 30 colonies were randomly selected and identified with sequencing.

2.6. Statistics

Statistical analysis was performed with GraphPad Prism 9, with an unpaired *t*-test or ANOVA under the default setting.

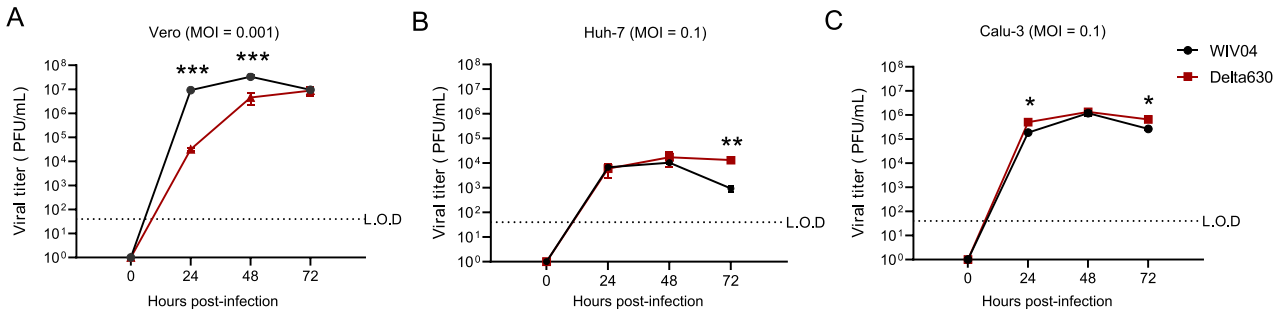

Fig. 1. Live virus replication in Calu-3 lung cells comparing SARS-CoV-2 B.1.617.2 Delta630 variant with the early strain WIV04. Growth curves of Delta630 and WIV04 in Vero (**A**), Huh-7 (**B**), and Calu-3 (**C**) cell lines at an MOI of 0.001, 0.1 and 0.1, respectively. The culture supernatant was collected at the indicated time point and virus titers were quantified in Vero-E6 cells by plaque assay. Triplicated titers of the two viruses in the cultures were analyzed by unpaired *t*-test. $*P < 0.05$; $**P < 0.01$; $***P < 0.001$. Dashed lines indicate the limit of detection (L.O.D).

3. Results

3.1. Delta variant shows enhanced infectivity in Huh-7 and Calu-3 cell lines

To characterize virus replication in cell culture, Vero cells were infected with Delta630 and WIV04 at MOI of 0.001, while Huh-7 and Calu-3 cells were infected at MOI of 0.1. As shown in Fig. 1, Delta630 replicated slower than WIV04 in Vero cells before 48 h post-infection (hpi), but reached the same level at 72 hpi; however, in Huh-7 cells, both viruses had similar growth before 48 hpi, but the titer of WIV04 at 72 hpi dropped significantly by 14-fold. In Calu-3 cells, a human lung cancer cell line, Delta630 showed minimally higher replication, which is consistent with previous studies showing that the D614G mutation in the spike protein increases infectivity in multiple human cell types (Zhang L. et al., 2020; Daniloski et al., 2021).

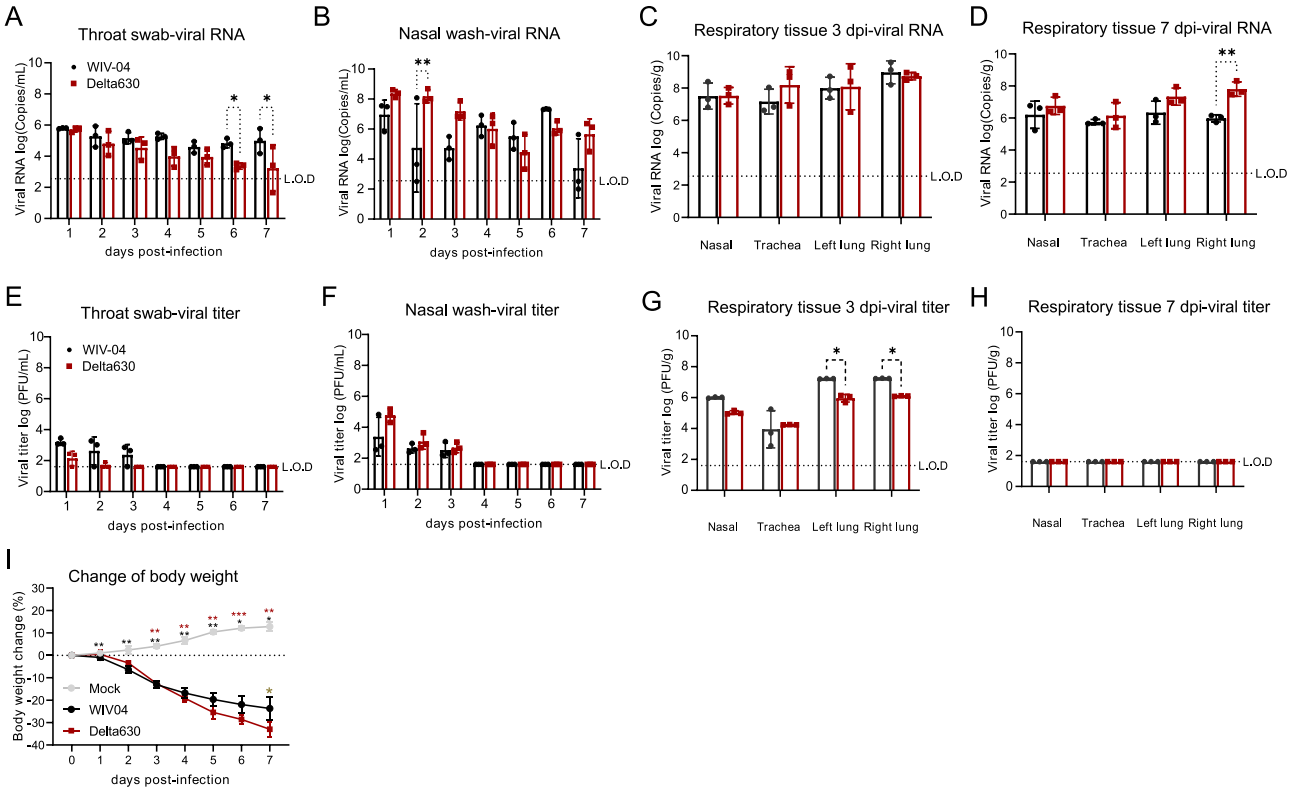

Fig. 2. The replication and pathogenicity of Delta630 and WIV04 in the Syrian hamster model. Hamsters were infected with 10^4 PFU of Delta630 and WIV04 (n = 6 for each group). Three hamsters were infected with the same volume of PBS as mock. The amount of viral RNA in the throat swab (**A**) and nasal wash (**B**) collected during seven days of observation, and tissue collected from animals euthanized on day 3 (**C**) and day 7 (**D**) post-infection were measured. The infectious virus titer in throat swab (**E**) and nasal wash (**F**) was detected during seven days of observation, and in tissues collected from animals euthanized on day 3 (**G**) and day 7 (**H**) post-infection were measured by plaque assay. The body weight (**I**) was monitored daily after viral infection. Statistically significant differences ($*P < 0.05$, $**P < 0.01$) were determined by two-way ANOVA followed by Tukey's multiple comparison test. Statistically significant differences versus uninfected hamsters are indicated as black and red asterisks, respectively for WIV04 and Delta630, while the significant diffference of weight loss in Delta630 versus WIV04 group at 7 dpi is marked with a brown asterisk. Dashed lines indicate the limit of detection (L.O.D).

3.2. Differential pathological abnormalities in the lungs caused by the Delta variant and WIV04 in hamsters

To investigate whether there is any difference in pathogenesis between Delta630 and WIV04, two groups of six hamsters were intranasally infected with 10^4 PFU of the two viruses. Viral RNA and infectious virus were detected up to 7 dpi in throat swab, nasal wash, nasal turbinate, trachea, and lung tissues (Fig. 2). In throat swab, WIV04 had slightly higher viral RNA than Delta630 from 2 dpi to 7 dpi, although statistical significance was detected only for 6 dpi and 7 dpi (Fig. 2A). Viral RNA in the nasal wash fluctuated for both WIV04 and Delta630, which may be due to the variation in the depth to which nasal washing reached the lungs, but higher viral RNA was detected for Delta630 on some days, especially at 2 dpi (Fig. 2B). Three animals were sacrificed on 3 dpi and 7 dpi in each group. At 3 dpi, no significant difference in viral RNA was observed between the nasal, tracheal, and lung samples (Fig. 2C). Consistent with RNA copies, slightly but not significantly more infectious virus was detected for WIV04 than Delta630 in throat swabs during the first 3 days after infection (Fig. 2E). However, the higher virus titers in the nasal wash were detected in hamsters infected with Delta630 without reaching a significant difference (Fig. 2F). At 3 dpi, significantly higher infectious virus was detected in the lungs for WIV04 than Delta630 by 30–120 folds (Fig. 2G). While the infectious virus was not detected in throat swabs, nasal washes collected after 3 dpi, or tissues collected on 7 dpi (Fig. 2H), more viral RNA was detected for Delta630 in the lung tissue on 7 dpi (Fig. 2D). After 3 dpi, hamsters showed significant weight loss compared with uninfected ones, and those infected with Delta630 experienced more loss than those infected with WIV04 (Fig. 2I), which was consistent with changes in viral load.

H&E staining of lung tissue indicated that the animals infected with Delta630 had a higher average histopathological score than those infected with WIV04 (Fig. 3A). The infiltration by inflammatory cells, mainly neutrophils and lymphocytes, was observed for both WIV04 and Delta630 around the bronchioles. Large areas of materialized alveolar walls were visible (black arrow), along with inflammatory cell infiltration (red arrow); around blood vessels, inflammatory cell infiltrates formed a vascular cuff (yellow arrow), and small bleeding was detected (green arrow). In contrast, a small amount of fibrin exudation was present in the alveolar cavity at the edge (blue arrow) in the lungs of Delta630 variant–infected hamsters, but not in the lung tissue infected with the WIV04 strain (Fig. 3B). Overall, more severe lung lesions, including consolidation, multifocal, and diffuse hyperemia, were seen in hamsters infected with Delta630 (Fig. 3C).

To further investigate the inflammatory response in the lung of the infected hamsters, mRNA levels of various inflammatory cytokines and chemokines were determined with RT-qPCR. SARS-CoV-2 infection resulted in the upregulated expression of cytokines such as IL-6, IL-10, IFN-λ, IFN-γ, IP-10, and MX-2, compared with noninfected hamsters (Fig. 4). Notably, compared with Delta630, WIV04 infection led to much higher expression of IP-10 and MX-2 on 3 dpi (Fig. 4F–G). Compared with mock, IFN-λ expression was most pronouncedly upregulated after infection (by hundreds fold) (Fig. 4H). In contrast, at 7 dpi, the expression levels of IL-10, IL-6, IP-10, MX2, and IFN-λ in the lungs infected with Delta630 remained at a relatively high level, which coordinated with the elevation of viral RNA at 7 dpi (Fig. 3). These results indicated that Delta630 infection resulted in more severe lung inflammation with a longer period of infection than WIV04.

3.3. The Delta variant leads to severe weight loss and partial mortality in hamsters

We investigated whether Delta630 was fatal to hamsters in a longer infection course after discovering that it generated more severe clinical outcomes and a prolonged illness course with a more extended period of increased viral and inflammatory response in the lungs. Hamsters were intranasally infected with Delta630 at the doses of 10^2, 10^3, 10^4, and 10^5

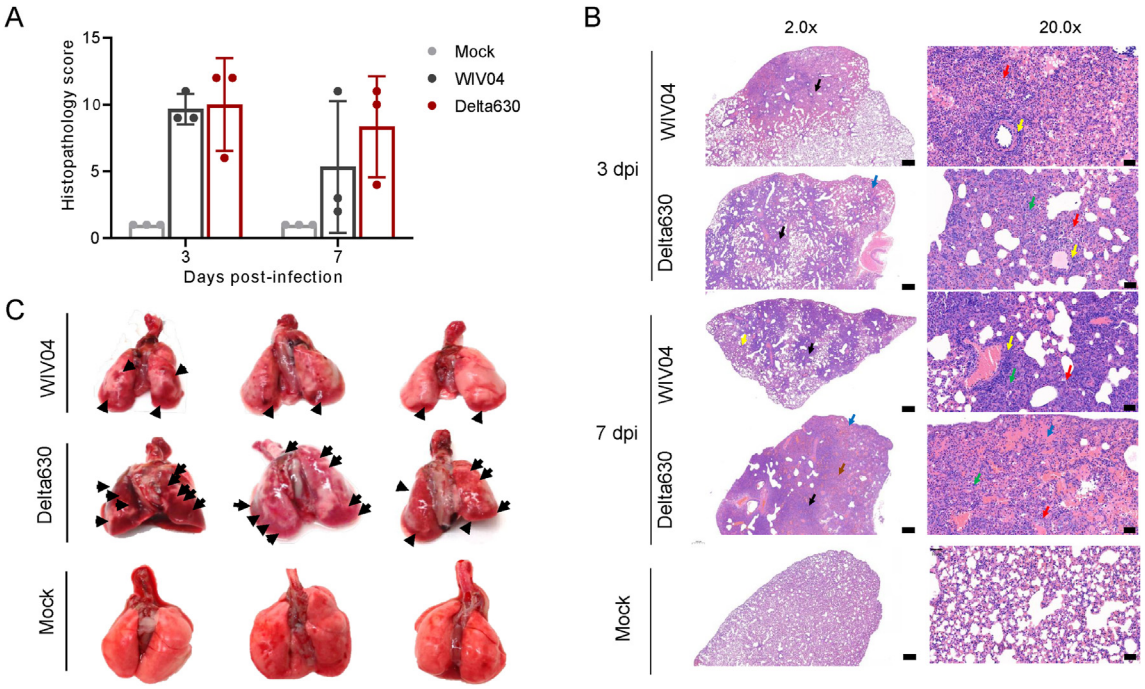

Fig. 3. The pathological examination of lung tissues after infection with Delta630 and WIV04. **A** Comprehensive pathological score of lung sections derived from hematoxylin and eosin (H&E) staining. Histologic lesion severity was scored according to a standardized scoring system evaluating the presence of interstitial pneumonia, type II pneumocyte hyperplasia, edema and fibrin, and perivascular lymphoid cuffing: 0, no lesions; 1, minimal (1%–10% of lobe affected); 2, mild (11%–25%); 3, moderate (26%–50%); 4, marked (51%–75%); 5, severe (76%–100%). **B** H&E staining of representative images in lung tissues at 3 and 7 dpi. Views of the lung lobes were shown in left panels (bar = 500 μm) and right panels (bar = 50 μm). Alveolar wall materialization (black arrow), inflammatory cell infiltration (red arrow), forming a vascular cuff (yellow arrow), fibrin exudation (blue arrow), and bleeding (green arrow). **C** More severe lung lesions including consolidation, multifocal, and diffuse hyperemia were seen in hamsters infected with Delta630 at 7 dpi.

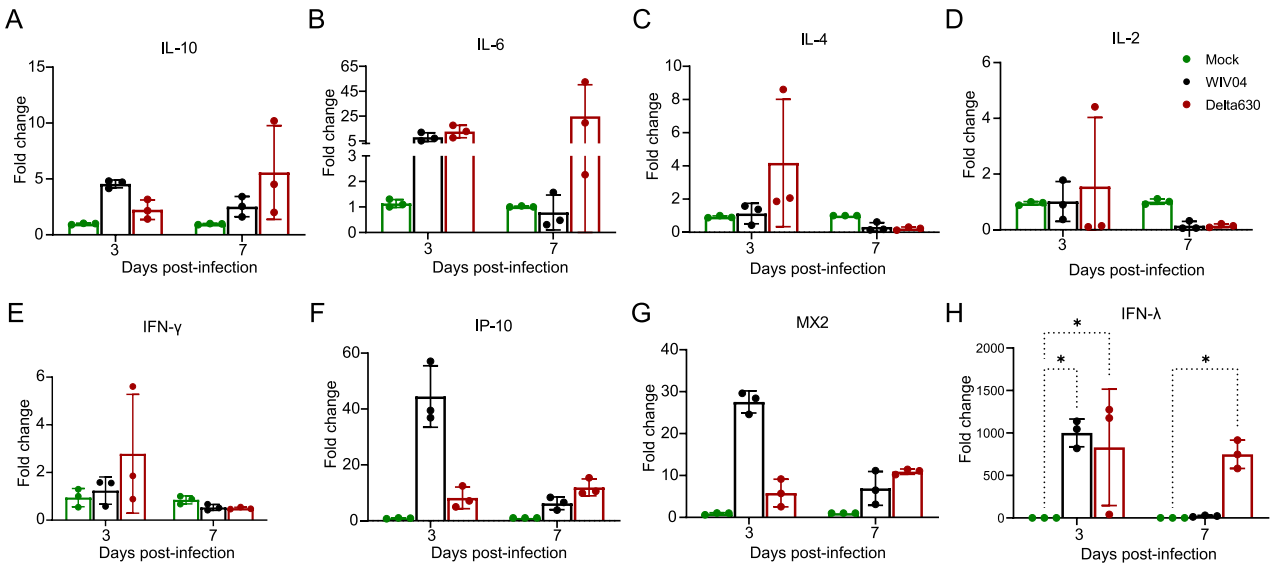

Fig. 4. The inflammatory response in the lung of infected hamsters. RNA levels for IL-10 (**A**), IL-6 (**B**), IL-4 (**C**), IL-2 (**D**), IFN-ɣ (**E**), IP-10 (**F**), MX2 (**G**), and IFN-λ (**H**) were determined by RT-qPCR in lung tissue of hamsters infected with WIV04 and Delta630 on day 3 and 7 post-infection, normalized for β-actin mRNA levels, and fold changes over the median of uninfected controls were calculated using the 2 (−ΔΔCt) method. Data presented as fold change over non-infected control (Mock). Statistical analyses were performed using two-way ANOVA followed by Tukey's multiple comparison test.

PFU; for comparison, a group of animals was infected with 10^5 PFU of WIV04. The animals kept losing weight until 6 to 7 dpi, as seen in Fig. 5A, at which point the surviving animals began to gain weight. The average maximum weight loss of the animals infected with Delta630 was 16.1%, 17.9%, 20.5%, and 8.7%, respectively for groups 10^5 PFU, 10^4 PFU, 10^3 PFU, and 10^2 PFU, while for those infected with 10^5 PFU of WIV04 was 14.1%. Unpredictably, in the 10^5 PFU and 10^4 PFU Delta630 groups, two of five hamsters died on 6 dpi and 7 dpi, and one of three in the 10^3 PFU Delta630 group died on 7 dpi; no death was observed for the 10^2 PFU Delta630 group and 10^5 PFU WIV04 group (Fig. 5B). The cumulative clinical scores were higher in hamsters infected with Delta630 than WIV04, though there was no significant difference (Fig. 5C).

We compared the pathogenicity of Delta630 with two other Delta strains, Delta84 and Delta85, as well as with the earlier strain WIV04 in hamsters to ascertain whether the biological characteristics of Delta630, particularly its lethality to hamsters, are specific to this strain or are shared by many Delta variants collectively. As shown in Supplementary Fig. S1, all four viruses caused significant body weight loss, but only Delta630 caused death, indicating that Delta630-induced hamster death was strain-specific.

3.4. Delta variant demonstrates increased airborne transmission competitiveness

Given that the SARS-CoV-2 Delta variant has increased transmissibility (Allen et al., 2022), we designed competitive airborne transmission experiments to elucidate the potential replication and transmission differences between Delta630 and WIV04. Three hamsters were intranasally inoculated with the 1:1 mixture of Delta630 and WIV04. On the next day, as donors, they were non-direct-contact cohoused for 1 h with three naive animals (sentinels), demonstrating 100% transmission in our settings. One day after infection or exposure, viral genomic RNA and infectious virus particles were found in the nasal wash of all the donors and sentinels; however, both levels drastically dropped in the latter (Fig. 6A and B), indicating 100% transmission in our settings. There was a clear trend of the decreasing proportion of Delta630 from the donors to the sentinels, while the proportion of WIV04 was decreasing in the transmission competition experiment (Fig. 6C). The ratio of the two viruses in each animal was determined by RT-PCR and colony sequencing. In one experiment (Chain 1 in Fig. 6D), the 50:50 ratio of Delta630 versus WIV04 in input turned into 60:40 in donor 1 and

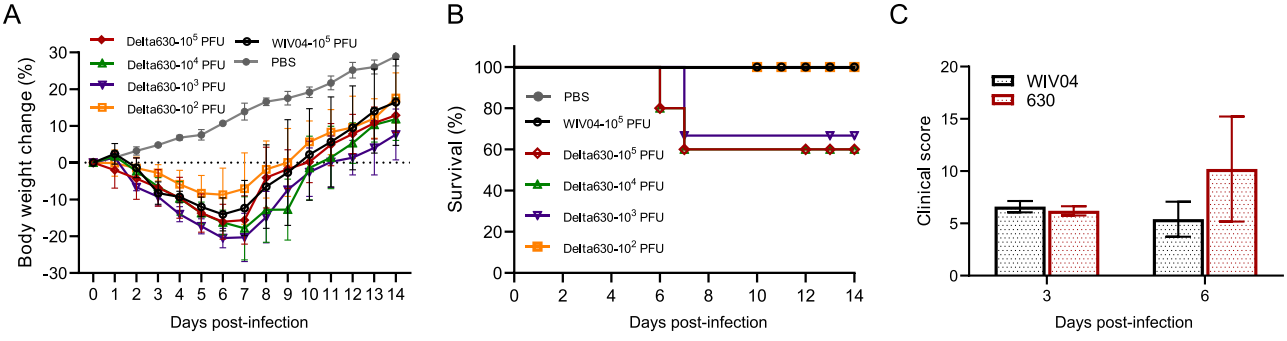

Fig. 5. The body weight loss and mortality of hamsters infected with Delta630 and WIV04. The animals were inoculated intranasally with serial 10-fold dilutions of Delta630 at dose of 10^2 PFU (n = 3), 10^3 PFU (n = 3), 104 PFU (n = 5), 10^5 PFU (n = 5), or WIV04 at 10^5 PFU (n = 5). Animals in the control group received PBS intranasally (n = 3). Body weight (**A**) and survival rate (**B**) were recorded until 14 dpi. **C** The clinical score on 3 and 6 dpi. Clinical symptom was scored based on the cumulative severity of symptoms including weight loss, posture, hunched, coat condition, shiny/ruffled, activity in cage, respiration, mobility, movements, and responses.

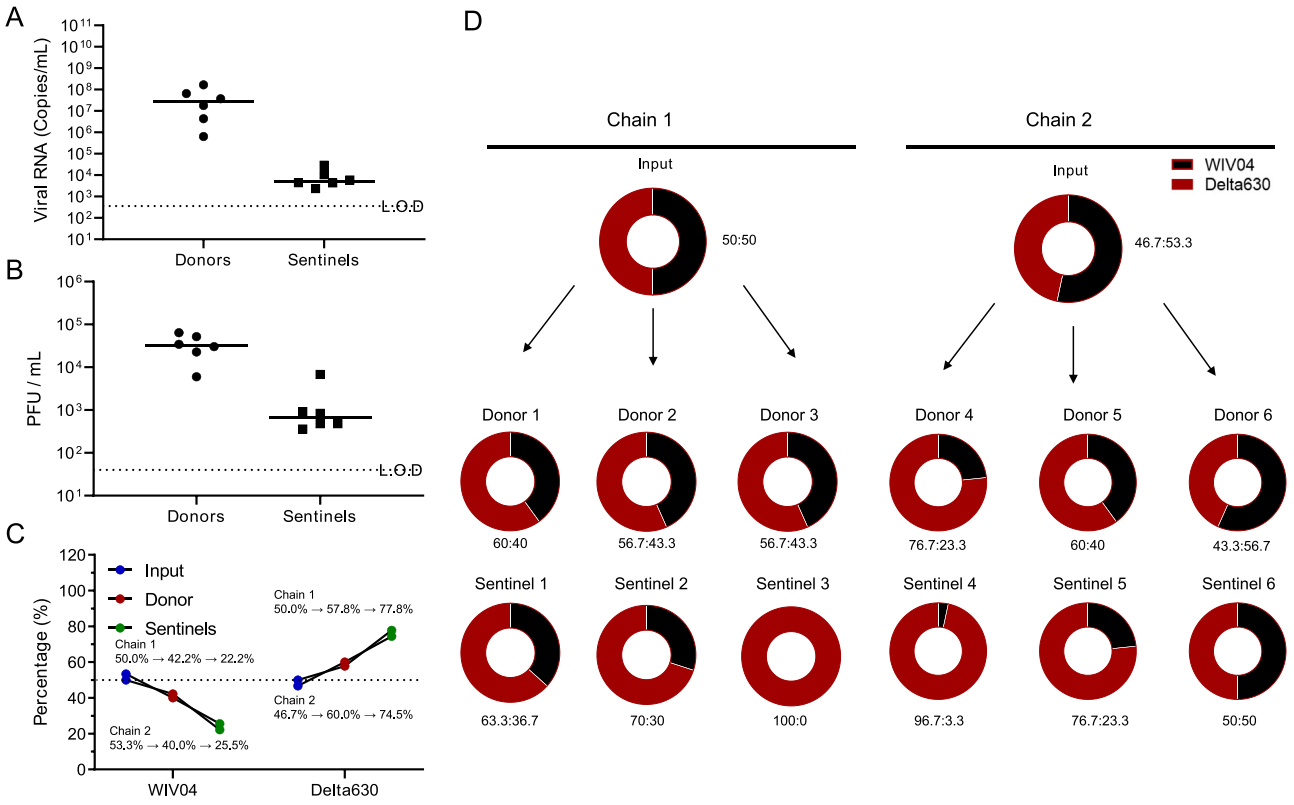

Fig. 6. Competitive airborne transmission experiment. Donor animals (n = 3) were infected with Delta630 and WIV04 at 10^4 PFU each via the intranasal route (1:1 ratio), and the next day three sentinels were exposed at 4 cm distance for one hour. Viral load in nasal wash of donors and sentinels collected 24 h post-infection/exposure was measured by genomic RNA (**A**) and tittered in Vero-E6 cells by plaque assays (**B**). **C** Percentage of Delta630 detected in inoculation and nasal wash collected from each individual donor and sentinel by Sanger sequencing. **D** Pie-charts depiction of the individual animal. Dashed lines indicate the limit of detection (L.O.D).

56.7:43.3 in donors 2 and 3, and then 63.3:36.7, 70:30, and 100:0 in Sentinels 1, 2, and 3, respectively. The increases of Delta630 were reproducible in another experiment (Chain 2), which started from a little less Delta630 with the ratio of 46.7:53.3, turning to 76.7:23.3, 60:40, and 43.3:56.7 for three donors and 96.7:3.3, 76.7:23.3, and 50:50 for three sentinels. The outcompetition of Delta630 over WIV04 demonstrated that Delta630 had increased airborne transmission.

4. Discussion

The emergence of SARS-CoV-2 Delta variants has posed a serious challenge to the public health system worldwide. Nevertheless, animal studies of the Delta variant are limited. In this study, we characterized risk element factors such as increased infectiousness, transmissibility, and mortality in hamsters. We found evidence of the increased airborne transmission competitiveness in hamsters infected with the Delta variant. Surprisingly, the SARS-CoV-2 Delta variant 630 strain can be partially lethal to some hamsters, even those infected with a dose of 10^3 PFU. A higher viral replication rate of Delta630 was confirmed *in vitro* in this study. Additionally, there was more virus shedding of Delta630 than WIV04 in the nasal wash of hamsters. Clinically, in newly diagnosed COVID-19 patients, the Delta variant has a higher viral load than historical variants in nasopharyngeal samples (Teyssou et al., 2021). According to Mohandas et al. (2021), 10^4 $TCID_{50}$ of the Delta variant causes minimal weight loss while inducing moderate illness in the lungs of around 40% of 8–10-week-old female hamsters. In our model of 4–6-week-old hamsters, 10^4 PFU of Delta630 caused severe lung disease and considerable weight loss in all animals. More importantly, hamsters infected with more than 10^3 PFU of Delta630 experienced death in 30%–40%. The difference might be accounted for by the variable virus strains and hamster ages. According to Abdelnabi et al. (2021), infected hamsters have a high expression of cytokines including IL-6, IFN-λ, IP-10, and MX2 in lung tissue after infection with SARS-CoV-2. Even though no infectious virus was found on 7 dpi, higher levels of IL-10, IL-6, IP-10, MX2, and IFN-λ were maintained in the lungs of hamsters infected with Delta630 than with WIV04 in this study. It has been reported that IL-6 and IP-10 are significantly higher in critical patients than in moderate and severe ones (Chen et al., 2020; Han et al., 2020), which is consistent with our results. All these results support the conclusion that Delta630 causes a more severe disease than WIV04.

SARS-CoV-2 can be transmitted efficiently from infected hamsters to naive hamsters by both direct contact and via aerosols (Sia et al., 2020). Using an airborne transmission model, Port et al. conducted a competitive transmissibility study and showed that B.1.1.7 variant outcompeted the lineage A variant (Port et al., 2022). With a similar strategy, we demonstrated that Delta630 had higher transmissibility than WIV04. Our data also suggest that the higher infectiousness of the B.1.617.2 Delta variant may not be due to the higher viral burden. According to some research, the spike protein in Delta is especially adept at membrane fusion and spike-mediated entry, which helps to explain why Delta spreads considerably more quickly after a brief exposure (Mlcochova et al., 2021; Zhang et al., 2021).

5. Conclusions

In summary, we herein presented a new SARS-CoV-2 Delta variant strain with enhanced virulence and transmissibility, and the strain was lethal to hamsters. To our knowledge, this is the first SARS-CoV-2 strain that causes death in a hamster model. By testing the SARS-CoV-2 B.1.617.2 Delta630 strain, we gained insight into the deadly hamster

model for examining severe or lethal COVID-19. In addition, the tissue tropism, host response, cell damage profiling, and molecular mechanism contributing to the high pathogenicity of Delta630 strain in hamsters remain to be investigated further. The viral characteristics of the Delta variant that we have supplied here are useful for a comparative analysis of the infectiousness of other newly emerging variants.

Data availability

All the data generated during the current study are included in the manuscript.

Ethics statement

This study was performed in strict accordance with the recommendations in the Guide for the Care and Use of Laboratory Animals of the Ministry of Science and Technology of the People's Republic of China. All hamster experiments were carried out at an animal biosafety level 3 (ABSL3) facility with the consent of the Animal Ethics Committee of the Wuhan Institute of Virology (WIVA45202104).

Author contributions

Xinghai Zhang: conceptualization, investigation, data curation, formal analysis, visualization, writing-original draft, writing-review & editing. Shaohong Chen: investigation, methodology. Zengguo Cao: investigation, methodology. Yanfeng Yao: investigation, methodology. Junping Yu: resources. Junhui Zhou: investigation. Ge Gao: investigation. Ping He: resources. Zhuo Dong: resources. Jie Zhong: resources. Jing Luo: resources. Hongping Wei: data curation, project administration, resources. Huajun Zhang: project administration, formal analysis, investigation, writing-review and editing, funding acquisition.

Conflict of interest

The authors declare that they have no conflict of interest.

Acknowledgements

We thank Jia Wu, Jun Liu, Hao Tang, Cheng Peng and others in the Wuhan National Biosafety Laboratory running team, including engineer, biosafety, biosecurity, and administrative staff for their technical assistance. We thank the Center for Biosafety Mega-Science, Chinese Academy of Sciences. We also thank the staff from National Virus Resource Center for material support. This work was supported by China Natural Science Foundation (82150201).

Appendix A. Supplementary data

Supplementary data to this article can be found online at https://doi.org/10.1016/j.virs.2022.09.008.

References

Abdelnabi, R., Boudewijns, R., Foo, C.S., Seldeslachts, L., Sanchez-Felipe, L., Zhang, X., Delang, L., Maes, P., Kaptein, S.J.F., Weynand, B., Vande Velde, G., Neyts, J., Dallmeier, K., 2021. Comparing infectivity and virulence of emerging SARS-COV-2 variants in Syrian hamsters. EBioMedicine 68, 103403.

Allen, H., Vusirikala, A., Flannagan, J., Twohig, K.A., Zaidi, A., Chudasama, D., Lamagni, T., Groves, N., Turner, C., Rawlinson, C., Lopez-Bernal, J., Harris, R., Charlett, A., Dabrera, G., Kall, M., 2022. Household transmission of COVID-19 cases associated with SARS-COV-2 delta variant (B.1.617.2): National case-control study. Lancet Reg Health Eur 12, 100252.

Chakraborty, C., Bhattacharya, M., Sharma, A.R., 2021. Present variants of concern and variants of interest of severe acute respiratory syndrome coronavirus 2: their significant mutations in S-glycoprotein, infectivity, re-infectivity, immune escape and vaccines activity. Rev. Med. Virol. 32, e2270.

Chan, J.F.W., Zhang, A.J., Yuan, S., Poon, V.K.M., Chan, C.C.S., Lee, A.C.Y., Chan, W.M., Fan, Z., Tsoi, H.W., Wen, L., Liang, R., Cao, J., Chen, Y., Tang, K., Luo, C., Cai, J.-P., Kok, K.H., Chu, H., Chan, K.H., Sridhar, S., Chen, Z., Chen, H., To, K.K.W., Yuen, K.Y., 2020. Simulation of the clinical and pathological manifestations of coronavirus disease 2019 (covid-19) in a Golden Syrian hamster model: implications for disease pathogenesis and transmissibility. Clin. Infect. Dis. 71, 2428–2446.

Chen, Y., Wang, J., Liu, C., Su, L., Zhang, D., Fan, J., Yang, Y., Xiao, M., Xie, J., Xu, Y., Li, Y., Zhang, S., 2020. IP-10 and MCP-1 as biomarkers associated with disease severity of COVID-19. Mol. Med. 26, 97.

Cucinotta, D., Vanelli, M., 2020. WHO declares COVID-19 a pandemic. Acta Biomed.: Atenei Parmensis. https://pubmed.ncbi.nlm.nih.gov/32191675. (Accessed 9 October 2022).

Dagpunar, J., 2021. Interim estimates of increased transmissibility, growth rate, and reproduction number of the COVID-19 B.1.617.2 variant of concern in the United Kingdom. medRxiv. https://doi.org/10.1101/2021.06.03.21258293.

Daniloski, Z., Jordan, T.X., Ilmain, J.K., Guo, X., Bhabha, G., tenOever, B.R., Sanjana, N.E., 2021. The spike D614G mutation increases SARS-CoV-2 infection of multiple human cell types. Elife 10, e65365.

Earnest, R., Uddin, R., Matluk, N., Renzette, N., Turbett, S.E., Siddle, K.J., Loreth, C., Adams, G., Tomkins-Tinch, C.H., Petrone, M.E., Rothman, J.E., Breban, M.I., Koch, R.T., Billig, K., Fauver, J.R., Vogels, C.B.F., Bilguvar, K., De Kumar, B., Landry, M.L., Peaper, D.R., Kelly, K., Omerza, G., Grieser, H., Meak, S., Martha, J., Dewey, H.B., Kales, S., Berenzy, D., Carpenter-Azevedo, K., King, E., Huard, R.C., Novitsky, V., Howison, M., Darpolor, J., Manne, A., Kantor, R., Smole, S.C., Brown, C.M., Fink, T., Lang, A.S., Gallagher, G.R., Pitzer, V.E., Sabeti, P.C., Gabriel, S., MacInnis, B.L., , New England Variant Investigation Team, Tewhey, R., Adams, M.D., Park, D.J., Lemieux, J.E., Grubaugh, N.D., 2022. . Comparative transmissibility of SARS-CoV-2 variants Delta and alpha in New England, USA. Cell Rep Med 3, 100583.

Feng, L., Wang, Q., Shan, C., Yang, C., Feng, Y., Wu, J., Liu, X., Zhou, Y., Jiang, R., Hu, P., Liu, X., Zhang, F., Li, P., Niu, X., Liu, Y., Zheng, X., Luo, J., Sun, J., Gu, Y., Liu, B., Xu, Y., Li, C., Pan, W., Zhao, J., Ke, C., Chen, X., Xu, T., Zhong, N., Guan, S., Yuan, Z., Chen, L., 2020. An adenovirus-vectored COVID-19 vaccine confers protection from SARS-CoV-2 challenge in rhesus macaques. Nat. Commun. 11, 1–11.

Fisman, D.N., Tuite, A.R., 2021. Progressive increase in virulence of novel SARS-CoV-2 variants in Ontario, Canada, February to June, 2021. medRxiv. https://doi.org/10.1101/2021.07.05.21260050.

Han, H., Ma, Q., Li, C., Liu, R., Zhao, L., Wang, W., Zhang, P., Liu, X., Gao, G., Liu, F., Jiang, Y., Cheng, X., Zhu, C., Xia, Y., 2020. Profiling serum cytokines in COVID-19 patients reveals IL-6 and IL-10 are disease severity predictors. Emerg. Microb. Infect. 9, 1123–1130.

Huang, K., Zhang, Y., Hui, X., Zhao, Y., Gong, W., Wang, T., Zhang, S., Yang, Y., Deng, F., Zhang, Q., Chen, X., Yang, Y., Sun, X., Chen, H., Tao, Y.J., Zou, Z., Jin, M., 2021. Q493K and Q498H substitutions in spike promote adaptation of SARS-CoV-2 in mice. EBioMedicine 67, 103381.

Imai, M., Iwatsuki-Horimoto, K., Hatta, M., Loeber, S., Halfmann, P.J., Nakajima, N., Watanabe, T., Ujie, M., Takahashi, K., Ito, M., Yamada, S., Fan, S., Chiba, S., Kuroda, M., Guan, L., Takada, K., Armbrust, T., Balogh, A., Furusawa, Y., Okuda, M., Ueki, H., Yasuhara, A., Sakai-Tagawa, Y., Lopes, T.J., Kiso, M., Yamayoshi, S., Kinoshita, N., Ohmagari, N., Hattori, S.I., Takeda, M., Mitsuya, H., Krammer, F., Suzuki, T., Kawaoka, Y., 2020. Syrian hamsters as a small animal model for SARS-CoV-2 infection and countermeasure development. Proc. Natl. Acad. Sci. USA 117, 16587–16595.

Konings, F., Perkins, M.D., Kuhn, J.H., Pallen, M.J., Alm, E.J., Archer, B.N., Barakat, A., Bedford, T., Bhiman, J.N., Caly, L., Carter, L.L., Cullinane, A., de Oliveira, T., Druce, J., El Masry, I., Evans, R., Gao, G.F., Gorbalenya, A.E., Hamblion, E., Herring, B.L., Hodcroft, E., Holmes, E.C., Kakkar, M., Khare, S., Koopmans, M.P., Korber, B., Leite, J., MacCannell, D., Marklewitz, M., Maurer-Stroh, S., Rico, J.A., Munster, V.J., Neher, R., Munnink, B.O., Pavlin, B.I., Peiris, M., Poon, L., Pybus, O., Rambaut, A., Resende, P., Subissi, L., Thiel, V., Tong, S., van der Werf, S., von Gottberg, A., Ziebuhr, J., Van Kerkhove, M.D., 2021. SARS-CoV-2 variants of interest and concern naming scheme conducive for global discourse. Nat. Microbiol. 6, 821–823.

Lee, C.Y., Lowen, A.C., 2021. Animal models for SARS-COV-2. Curr. Opin. Virol. 48, 73–81.

Li, B., Deng, A., Li, K., Hu, Y., Li, Z., Shi, Y., Xiong, Q., Liu, Z., Guo, Q., Zou, L., Zhang, H., Zhang, M., Ouyang, F., Su, J., Su, W., Xu, J., Lin, H., Sun, J., Peng, J., Jiang, H., Zhou, P., Hu, T., Luo, M., Zhang, Y., Zheng, H., Xiao, J., Liu, T., Tan, M., Che, R., Zeng, H., Zheng, Z., Huang, Y., Yu, J., Yi, L., Wu, J., Chen, J., Zhong, H., Deng, X., Kang, M., Pybus, O.G., Hall, M., Lythgoe, K.A., Li, Y., Yuan, J., He, J., Lu, J., 2022. Viral infection and transmission in a large, well-traced outbreak caused by the SARS-CoV-2 Delta variant. Nat. Commun. 13, 460.

Liu, Y., Rocklöv, J., 2021. The reproductive number of the Delta variant of SARS-COV-2 is far higher compared to the ancestral SARS-CoV-2 virus. J. Trav. Med. 28 taab124.

Mlcochova, P., Kemp, S.A., Dhar, M.S., Papa, G., Meng, B., Ferreira, I.A.T.M., Datir, R., Collier, D.A., Albecka, A., Singh, S., Pandey, R., Brown, J., Zhou, J., Goonawardane, N., Mishra, S., Whittaker, C., Mellan, T., Marwal, R., Datta, M., Sengupta, S., Ponnusamy, K., Radhakrishnan, V.S., Abdullahi, A., Charles, O., Chattopadhyay, P., Devi, P., Caputo, D., Peacock, T., Wattal, C., Goel, N., Satwik, A., Vaishya, R., Agarwal, M., Indian SARS-CoV-2 Genomics Consortium (INSACOG); Genotype to Phenotype Japan (G2P-Japan) Consortium; CITIID-NIHR BioResource COVID-19 Collaboration, Mavousian, A., Lee, J.H., Bassi, J., Silacci-Fegni, C., Saliba, C., Pinto, D., Irie, T., Yoshida, I., Hamilton, W.L., Sato, K., Bhatt, S., Flaxman, S., James, L.C., Corti, D., Piccoli, L., Barclay, W.S., Rakshit, P., Agrawal, A., Gupta, R.K., 2021. SARS-CoV-2 B.1.617.2 Delta variant replication and immune evasion. Nature 599, 114–119.

Mohandas, S., Yadav, P.D., Shete, A., Nyayanit, D., Sapkal, G., Lole, K., Gupta, N., 2021. SARS-CoV-2 delta variant pathogenesis and host response in Syrian hamsters. Viruses 13, 1773.

Port, J.R., Yinda, C.K., Avanzato, V.A., Schulz, J.E., Holbrook, M.G., van Doremalen, N., Shaia, C., Fischer, R.J., Munster, V.J., 2022. Increased small particle aerosol transmission of B.1.1.7 compared with SARS-CoV-2 lineage a in vivo. Nat. Microbiol. 7, 213–223.

Port, J.R., Yinda, C.K., Owusu, I.O., Holbrook, M., Fischer, R., Bushmaker, T., Avanzato, V.A., Schulz, J.E., Martens, C., van Doremalen, N., Clancy, C.S., Munster, V.J., 2021. SARS-CoV-2 disease severity and transmission efficiency is increased for airborne compared to fomite exposure in Syrian hamsters. Nat. Commun. 12, 1–15.

Rosenke, K., Meade-White, K., Letko, M., Clancy, C., Hansen, F., Liu, Y., Okumura, A., Tang-Huau, T.L., Li, R., Saturday, G., Feldmann, F., Scott, D., Wang, Z., Munster, V., Jarvis, M.A., Feldmann, H., 2020. Defining the Syrian hamster as a highly susceptible preclinical model for SARS-CoV-2 infection. Emerg. Microb. Infect. 9, 2673–2684.

Sia, S.F., Yan, L.M., Chin, A.W., Fung, K., Choy, K.T., Wong, A.Y., Kaewpreedee, P., Perera, R.A., Poon, L.L., Nicholls, J.M., Peiris, M., Yen, H.-L., 2020. Pathogenesis and transmission of SARS-CoV-2 in golden hamsters. Nature 583, 834–838.

Sun, S.H., Chen, Q., Gu, H.J., Yang, G., Wang, Y.X., Huang, X.Y., Liu, S.S., Zhang, N.N., Li, X.F., Xiong, R., Guo, Y., Deng, Y.Q., Huang, W.J., Liu, Q., Liu, Q.M., Shen, Y.L., Zhou, Y., Yang, X., Zhao, T.Y., Fan, C.F., Zhou, Y.S., Qin, C.F., Wang, Y.C., 2020. A mouse model of SARS-CoV-2 infection and pathogenesis. Cell Host Microbe 28, 124–133 e124.

Sun, S., Gu, H., Cao, L., Chen, Q., Ye, Q., Yang, G., Li, R.T., Fan, H., Deng, Y.-Q., Song, X., Qi, Y., Li, M., Lan, J., Feng, R., Guo, Y., Zhu, N., Qin, S., Wang, L., Zhang, Y.F., Zhou, C., Zhao, L., Chen, Y., Shen, M., Cui, Y., Yang, X., Wang, X., Tan, W., Wang, H., Wang, X., Qin, C.F., 2021. Characterization and structural basis of a lethal mouse-adapted SARS-CoV-2. Nat. Commun. 12, 1–16.

Teyssou, E., Delagrèverie, H., Visseaux, B., Lambert-Niclot, S., Brichler, S., Ferre, V., Marot, S., Jary, A., Todesco, E., Schnuriger, A., Ghidaoui, E., Abdi, B., Akhavan, S., Houhou-Fidouh, N., Charpentier, C., Morand-Joubert, L., Boutolleau, D., Descamps, D., Calvez, V., Marcelin, A.G., Soulie, C., 2021. The delta SARS-CoV-2 variant has a higher viral load than the beta and the historical variants in nasopharyngeal samples from newly diagnosed COVID-19 patients. J. Infect. 83, e1–e3.

Twohig, K.A., Nyberg, T., Zaidi, A., Thelwall, S., Sinnathamby, M.A., Aliabadi, S., Seaman, S.R., Harris, R.J., Hope, R., Lopez-Bernal, J., 2021. Hospital admission and emergency care attendance risk for SARS-CoV-2 delta (B. 1.617. 2) compared with alpha (B.1.1.7) variants of concern: a cohort study. Lancet Infect. Dis. 22, 35–42.

World Health Organization (WHO), 2022a. Weekly Epidemiological Update on COVID-19 - 7 September 2022. https://www.who.int/publications/m/item/weekly-epidemiological-update-on-covid-19—7-september-2022. (Accessed 7 September 2022).

World Health Organization (WHO), 2022b. Tracking SARS-CoV-2 Variants. https://www.who.int/en/activities/tracking-SARS-CoV-2-variants/. (Accessed 11 August 2022).

Zhang, J., Xiao, T., Cai, Y., Lavine, C.L., Peng, H., Zhu, H., Anand, K., Tong, P., Gautam, A., Mayer, M.L., Walsh, R.M., Rits-Volloch, S., Wesemann, D.R., Yang, W., Seaman, M.S., Lu, J., Chen, B., 2021. Membrane fusion and immune evasion by the spike protein of SARS-CoV-2 delta variant. Science 374, 1353–1360.

Zhang, L., Jackson, C.B., Mou, H., Ojha, A., Peng, H., Quinlan, B.D., Rangarajan, E.S., Pan, A., Vanderheiden, A., Suthar, M.S., Li, W., Izard, T., Rader, C., Farzan, M., Choe, H., 2020. SARS-COV-2 spike-protein D614G mutation increases virion spike density and infectivity. Nat. Commun. 11, 6013.

Zhang, Q., Zhang, H., Gao, J., Huang, K., Yang, Y., Hui, X., He, X., Li, C., Gong, W., Zhang, Y., Zhao, Y., Peng, C., Gao, X., Chen, H., Zou, Z., Shi, Z.-L., Jin, M., 2020. A serological survey of SARS-CoV-2 in cat in Wuhan. Emerg. Microb. Infect. 9, 2013–2019.

Zhou, P., Yang, X.L., Wang, X.G., Hu, B., Zhang, L., Zhang, W., Si, H.R., Zhu, Y., Li, B., Huang, C.L., Chen, H.D., Chen, J., Luo, Y., Guo, H., Jiang, R.-D., Liu, M.Q., Chen, Y., Shen, X.-R., Wang, X., Zheng, X.-S., Zhao, K., Chen, Q.J., Deng, F., Liu, L.L., Yan, B., Zhan, F.X., Wang, Y.Y., Xiao, G.F., Shi, Z.L., 2020. A pneumonia outbreak associated with a new coronavirus of probable bat origin. Nature 579, 270–273.